DEVELOPMENT AND CHARACTERIZATION OF A MULTI-CELLULAR *IN VITRO* MODEL FOR THE STUDY OF NANOPARTICLE-CELL INTERFACE

by

Reinaldo Javier Agostini Infanzón

A thesis submitted in partial fulfillment of the requirements for the degree of

MASTER OF SCIENCE
in
MECHANICAL ENGINEERING

UNIVERSITY OF PUERTO RICO
MAYAGÜEZ CAMPUS
2018

Approved by:

Pedro Resto, Ph.D. President, Graduate Committee	Date
Maribella Domenech, Ph.D. Co-President, Graduate Committee	Date
Rubén Díaz, Ph.D. Member, Graduate Committee	Date
Oscar Perales, Ph.D. Office of Graduate Studies Representative	Date
Néstor Pérez, Ph.D. Chairperson of the Department	Date

ABSTRACT

Triple Negative Breast Cancer (TNBC) is distinguished by various characteristics which are associated to its poor prognosis. This type of cancer is aggressive in nature and has no targeted therapies. The tumor microenvironment has shown to modulate tumor cell behavior and response to clinical therapies. Current *in vitro* technologies allow us to observe multicellular interactions for extended periods; however, these present a variety of limitations including the need for cell sorting, requirement of large amounts of cells, and lack of tunable discrete adjacent compartments. Other technologies such as microfluidic platforms lack a user-friendly interface and require specialized instrumentation and training, making it difficult to be routinely used in a cell biology laboratory. To overcome these problems, an open multi-microwell triculture device was manufactured to probe tumor-stromal interactions. The devices were printed out of polystyrene sheets using a razor-blade plotter and manually layered into a 3-dimensional structure. We have evaluated the effect of normal and cancerous stromal cell clusters (fibroblasts and macrophages) in modulating tumor behavior in MDA-MB-231 cells. Tumor cell proliferation was evaluated at 72hrs cultured with stromal clusters under exposure to stress conditions. Results for normal stromal cell clusters show no significant difference in proliferation at 37°C and 41°C. On the other hand, cancer associated cells show an increased proliferation rate of 11.7% for 37°C than for 41°C. Normal stroma shows potential damping on the effects of the high temperature stress on the cells, as no significant difference was observed. Thus, normal stroma improves recovery from heat damage as compared to cancer-stroma. Multi-adjacent microwell stickers are a fast

prototyping culture platform and provide flexibility for testing diverse biomaterials with varying conditions for each cell type in multi-culture cell signaling studies.

RESUMEN

El cáncer de mama triple negativo (TNBC, por sus siglas en inglés) se distingue por varias características asociadas con su mal pronóstico. Este tipo de cáncer es de naturaleza agresiva y no tiene terapias dirigidas. El microambiente del tumor ha demostrado modular el comportamiento de las células tumorales y la respuesta a las terapias clínicas. Las tecnologías *in vitro* actuales nos permiten observar interacciones multicelulares durante períodos prolongados; sin embargo, éstos presentan una variedad de limitaciones que incluyen la necesidad de clasificación celular, el requerimiento de grandes cantidades de células y la falta de compartimentos adyacentes discretos sintonizables. Otras tecnologías, como las plataformas de microfluidos, carecen de una interfaz fácil de usar y requieren instrumentación y capacitación especializadas que dificultan su uso rutinario en un laboratorio de biología celular. Para superar estos problemas, se fabricó un dispositivo abierto de tricultura de pozos para probar las interacciones tumor-estromal. Los dispositivos se imprimieron en láminas de poliestireno utilizando un trazador con navaja y se colocaron en capas manualmente en una estructura tridimensional. Hemos evaluado el efecto de agrupaciones de células estromales normales y cancerosas (fibroblastos y macrófagos) en la modulación del comportamiento tumoral en células MDA-MB-231. La proliferación de células tumorales se evaluó a las 72 horas cultivadas con grupos de estroma bajo exposición a condiciones de estrés. Los resultados para los grupos de células estromales normales no muestran diferencias significativas en la proliferación a 37°C y 41°C. Por otro lado, las células asociadas con el cáncer muestran una tasa de proliferación aumentada de 11.7% para

37°C que para 41°C. El estroma normal muestra una posible amortiguación sobre los efectos del estrés por alta temperatura en las células, ya que no se observaron diferencias significativas. Por lo tanto, el estroma normal mejora la recuperación del daño por calor en comparación con el estroma del cáncer. Los dispositivos de múltiples pocillos son una plataforma rápida de prototipos y proporcionan flexibilidad para probar diversos biomateriales con diferentes condiciones para cada tipo de célula en estudios de señalización celular multicultural.

Table of Contents

Table of Figures

1 CHAPTER – INTRODUCTION

Magnetic Fluid Hyperthermia (MFH) has been shown to be a potential treatment against tumors. It consists of localized heat dissipation by magnetic nanoparticles in the tissue stimulated by an alternating magnetic field. Although results in tumor cells and animal models are promising, the effect of the tumor stroma is suspected to influence cell apoptosis and/or recovery post-MFH treatment.[1,2] The interactions between the cellular components of the tumor microenvironments are complex and are capable of shifting tumor progression and therapeutic outcomes.[3–5] These cellular interactions are potentially mediated by soluble factors secreted as a response to contact with magnetic nanoparticles and heat dissipation.[6,7] Thus, studies aimed to evaluate influence of cell-MNPs interactions and MFH in a multi-cellular microenvironment are needed to optimize MFH treatment to enhance cell selectivity and favor tumor cell apoptosis instead of a tissue healing response.

Multi-compartment microscale culture platforms are suitable for multi-cell type studies. Several studies show that *in vitro* models in microscale devices can recapitulate invasive and paracrine signaling observed in tissue level interactions, supporting their value for tumor biology.[8] *In vitro* model that can recapitulate *in vivo* interactions reduce the costs and complexity of associated to animal models and thereby are essential for optimization of therapies and biological studies. These would reduce cost of *in vivo* monitoring during early stages of biological modeling, allow otherwise unobservable situations amongst cells and materials, permit researchers to pinpoint and solve unique

difficulties for drug delivery, their effects and dosages, the engineering of synthetic interactions (e.g. biosensors) and allowing the observation of interactions between various types of cells.[9]

This research project is focused on the characterization of a multi-well culture platform for evaluation of multi-cell type contributions in the sensitivity of tumor cells to magnetic fluid hyperthermia. A multi-cell type model with triple-negative breast cancer cells was characterized using a custom designed microfluidic platform to provide an environment suitable for soluble factor interactions between cancer cells and the adjacent stroma. This thesis consists of a review of the scientific literature in Chapter 2, justification for the research in Chapter 3, objectives in Chapter 4, and the methodologies for the research are given in Chapter 5. The results are provided in Chapter 6.

2 CHAPTER – LITERATURE REVIEW

2.1 Triple Negative Breast Cancer

Triple Negative Breast Cancer (TNBC), typically most abundant in young African-American women and Hispanic women, is characterized by various attributes which are associated to its poor prognosis. First, the lack of estrogen (ER) and progesterone receptors (PR) and second, no human epidermal growth factor receptors (HER2) present either. This type of cancer is aggressive in nature and has no targeted therapies. Less than 30% of patients will survive a 5-year remission rate with standard therapy, especially Hispanic and African-American women where TNBC is more frequent and has the lowest (<14%) survival rates.[1] Current potential therapeutic strategies for TNBC include androgen receptor targeted agents, epidermal growth factor receptor-targeted agents, anti-antigenic agents, and poly ADP ribose polymerase enzyme inhibitors. However, their uses as of date are limited to clinical trials and more work is necessary to identify targets which could yield significant advances in tumor regression and relapse.[10,11]

In various types of cancer, tumor progression is supported by the cellular composition of a pro-tumorigenic niche leading to an unresolved inflammatory response. This generally occurs via the localized accumulation of stromal cells followed by a loss of the means to maintain homeostasis.[6,12] A greater than predicted tumor incidence was observed for various types of cancer when analyzing 25,914 samples of female immunosuppressed organ transplant recipients. This included lung, gastrointestinal, reproductive, and skin cancer. On the other hand, the incidence of breast cancer decreased within this final cluster.[13] These differences imply a robust influence the

abundance of cellular sub-types present in the tumor microenvironment has alongside the development and/or suppression of tumor advancement.

2.2 MNP Potential for Treatment of TNBC

MFH is driven by heat dissipation from the surface of superparamagnetic MNPs in response to an alternating magnetic field (AMF). Heat dissipation is driven mainly by Néel relaxation and partially by Brown relaxation of magnetic core in response to the frequency of the magnetic field. Brown refers to the physical movement of the MNPs within a liquid, causing friction of the MNPs against the fluid. On the other hand, Néel relaxation consists in the reorientation of the magnetic moment within the MNPs upon exposure to an AMF.[14] Both relaxation effects increase the immediate liquid's temperature. This heat dissipation allows for heating of localized areas or volumes within tissues.

MNPs have been extensively studied for cancer therapy. Studies use a combination of currently existing therapies and nanoparticles for enhancing the effect of these. Nanoparticles can be polymer based, metal based, functionalized, and more, effectively proving that these are a flexible platform from which to establish a complex and comprehensive set of tools to combat disease.[15] MNP are promising in several biomedical applications in areas such as cellular therapy involving cell labeling plus targeting, as a tool for research used to separate and purify cell populations, tissue repair, targeted drug delivery, magnetic resonance imaging (MRI), and MFH for targeted cancer treatment.[15] Amongst the various types of MFH-capable MNP are iron cobalt, iron nickel, iron platinum, and iron oxide. Iron cobalt MNP are well known but present slight issues regarding its stability and ease of oxidation, which could negatively affect its

biocompatibility when in contact with cells. Iron nickel MNP are generally used for MRI but have been considered for clinical applications, particularly MFH. Iron platinum are generally very stable within solutions, show superparamagnetisation, have demonstrated good biocompatibility, and are used as contrast agents for MRI.[16–18] The most studied and well-known type is iron oxide MNP, where its interactions with cells an tissue can significantly vary depending on the type of conjugation made to it.[19] These have shown excellent biocompatibility, superparamagnetisation, effective colloidal stability, are also used as contrast agents for MRI, have been used as chemotherapy and radiotherapy enhancement agents, and various *in vivo* studies have been performed in animals such as rats, dogs, rabbits and clinical trials in humans.[16,19–21]

Previous works have taken advantage of the association of iron oxide MNP with cells by traveling across the cell membrane or becoming internalized into cellular compartments. Studies in metastatic TNBC cells (MDA-MB-231 cell line) have shown that receptor targeted MNPs promote permeabilization of lysosomal membranes to contribute to effectively causing cell apoptosis.[22] Thus, the efficacy of MFH is dependent on MNP stability and tumor uptake, and heat dissipation. To achieve enough tumor uptake of MNPs for optimal therapeutic outcome, certain parameters have been established to achieve improved blood circulation times, greater tumor uptake of MNP, and increased localized heating through MFH. MNP core size is a parameter that greatly influences its cellular uptake and magnetic properties. A magnetic core of 10-50 nm enables a single magnetic domain and, above a specific temperature, displays superparamagnetic behavior. Essentially, when the external magnetic field is removed, the particle's

magnetization is non-existent. This type of behavior contributes to colloidal stability within biological fluids (e.g. blood) and a quick response to applied magnetic fields with negligible remanence and coercivity.[19] Surface coatings, such as carboxymethyl dextran, further support colloidal stability in aqueous solutions and provide binding sites for cell targeting. This type of polymer coating also extends the blood circulation time of the MNPs, allowing for increased treatment windows, and consistent MNP concentrations within the treatment site.[15,23] In addition to colloidal stability, the response must be accompanied with high saturation magnetization, as it is directly associated with a larger thermal energy dissipation and a greater control on MNP movement within the tissue under an external magnetic field.[22,24] Other parameters for MNPs include biocompatibility, ease of escape from the reticuloendothelial system, and minimal protein adsorption, amongst others.[14] Superparamagnetic iron oxide MNPs fill these requirements and have been thoroughly studied regarding their use as a treatment and drug carriers.[25]

MNPs show great potential for a large amount of clinical treatments and therapies, particularly in drug delivery and MFH. However, challenges such as lack of technologies for frequent monitoring of cell-MNPs interactions in animals, *in vivo* toxicity, particle focusing via magnetic fields, and high blood circulation times (single day) remain to be addressed.[11,26,27]

2.3 MFH: Therapeutic Potential and Challenges

MFH has shown promising advances for the treatment of endocrine tumors. Consisting in production of localized heat by magnetic relaxation mechanisms, MFH depends on MNPs placed within a tumor where localized heat is produced under an alternating magnetic field (AMF) through magnetic relaxation mechanisms. MFH has been demonstrated to be capable of reducing cell viability, proliferation and survival factors of tumor cells *in vitro*[6] and tumor size reduction and prevention of metastasis *in vivo,* within immunocompromised mice and hamsters.[7,19] Some of the mechanisms have been known to contribute to the efficacy of MFH include lysosomal membrane permeabilization, proteasomal stress,[6,12] and synergistic effects when combined with cytotoxic drugs[28]. Gene expression has been measured upon exposure to MFH and one consequence is the upregulation of heat shock proteins, such as HSP70, which contributes to recovery of tumors and their resistance to treatment. Inhibition of this protein showed decreased cell viability after MFH treatment. These treatments were also performed within mouse models and likewise showed promising results.[7] Despite promising results, certain challenges remain to be addressed before reaching clinical environment clinic. MFH's therapeutic application in the clinic faces several challenges, including the need of field and frequency optimizations, better understanding of thermal effects on tissues, and surface modifications on MNPs.[29]

One major challenge of MFH is the limited amount of nanoparticles that reach the tumor, diminishing the overall heat dissipated within the tumor tissue.[30] This is a common issue among MNP systems, particularly those with surface charges. Macrophages

interact with MNPs by sequestering the particles and transporting them to locations such as the spleen and liver, leading to decreased blood circulation times.[30,31] However, these cells can also deliver MNPs to the bulk tumor tissue, increasing its local concentration at the tumor site.[32] Thus, macrophages are important determinants in the efficacy of MFH in tissues. Unfortunately, most studies have excluded these cells from murine models and current *in vitro* studies have been focused on MNP-tumor cell interactions, limiting our understanding of how these cells influence MFH.

Here we propose to use a multi-cellular *in vitro* culture model for evaluation of the influence of macrophages and other cellular components in the efficacy of MFH using iron oxide MNP.

2.4 Multi-cellular microscale culture platform for optimization of MFH

Biochemical communication between cancer and healthy cells still exists as each continues to excrete soluble signaling molecules. This communication is mainly influenced by soluble parameters, contributing to drug resistance. Tumor cells block influx of drug and may also alter genetic expression profiles upon exposure to treatments.[4,33] In order to determine the impact of multiple cell-cell interactions in therapeutic response of tumor cells, multi-cellular *in vitro* models are needed where, exposure to MFH treatments and multi-cellular communication can be simultaneously studied and each cell type can be independently observed and retrieve at multiple time points.

Various co-culture platforms and cellular models have been developed for the study of tumor-stromal interactions. Amongst these are cell suspensions, where one cell

population adhered to a solid support, and another suspended in liquid using conventional well plates.[34] Another model is multicellular spheroids, which consist as a 3D multicellular model serve for some structure, morphology, and deep imaging. Both models, which are very common amongst cancer studies, can be used for cell communication studies, although these do not allow obtain independent cell population read-outs. To evaluate cell specificity and efficacy of MNP in a multi-cellular system each cell population needs to be integrated during culture but analyzed independently. A brief overview of multi-cellular culture platforms reveals a limited number of publications in which three or more cell types are used for *in vitro* studies. Most culture platforms used for multicellular models used either mixed or compartmentalized cell culture approaches using a well or a microfluidic culture platform. In traditional well-plate culture, most models consist of a mixed culture approach except in cases where a suspended platform within a well, such as a Transwell, is utilized. In microfluidic platforms, a 3D vascularized microfluidic quad-culture assay are used to study metastasis within a bone-mimicking microenvironment. In such models, breast cancer cells thrive within microvascular networks generated by mural-like cells supported by endothelial and skeletal muscle cells.[35] A multi-cellular model of perfused 3D tri-culture model also exists for human breast cancer.[36] Stromal and breast cancer cells are seeded on top of a microtubule network, embedded within a tumor-aligned matrix, and later on, recruited into the stromal-breast cancer spheroid.[37] Although these culture models are relatively straightforward to manufacture, manipulation of samples to achieve independent cell type readouts is difficult particularly due to the poor accessibility to cell compartments and multi-step cell separation processes. Additional multi-culture models include a tri-culture platform to assess interactions

between osteoblasts, osteoclasts, and endothelial cells using commercially available, non-customizable polystyrene cell culture inserts.[38] A platform also exists for measuring drug treatment survival in a perfused 3D microfluidic culture platform using stromal cells, osteoblasts, and leukemic cells embedded within a 3-D collagen matrix.[39] Another model uses agarose to fix cells and to split a well into two, providing a non-mixed tri-culture model with discrete compartments.[40] Finally, another platform is a PDMS-based model of a bronchiole to study interaction within a lung between a host, its microenvironment, and a pathogen. This platform allows tri-culture and two additional microbial populations to interact with each other directly and indirectly.[41] Although these multicellular models provide valuable information about the biology of the different diseases, the manufacturing procedure, cell seeding dynamics, and accessibility to compartments, they represent constraints in the implementation of multicellular culture models within the broad scientific community. From amongst the microfluidic platforms available, even fewer are utilized for *in vitro* multi-culture MFH studies. One study used iron oxide MNPs under an AMF for treatment of murine metastatic mammary carcinoma cells in a spherical 3D co-culture mix with murine tumor endothelial cells, and murine embryonic fibroblasts. After MFH, cells showed increased cell death and mechanical disintegration which subsequently modified the cellular microenvironment.[18]

Microscale technologies have been successfully used in cell biology applications and biomedical studies. Previous work from our laboratory with paracrine Hh signaling and cell differentiation shows that microscale technologies provide an interface with the ability to mix and match cells in spatiotemporal controlled micro-compartments where a

diffusion-dominant environment under no-flow conditions enhances cell-cell communication via secreted factors.[42] This device design also enables the evaluation of multi-cellular signaling on cellular behavior (e.g. growth, gene expression). In our lab, Domenech *et al.* studies suggest that flow-less microchannel cultures lead to easier soluble factor signaling studies which "allows for an exploration of the stochastic effects of cell heterogeneity via studies that utilize hundreds of cells" instead of population-based studies which would require thousands to millions of cells or single cell analyses.[43] Compartmentalized microculture arrays enable multi-cell communication and independent cell-type endpoints.[44] The use of *n* adjacent microwells in a culture platform supports co-culture of multiple cell types in a 96-well plate format for automated read-outs. Cell proliferation, gene expression and MNP uptake can be independently evaluated for each cell type which will provide valuable information regarding the cell/nanoparticle interface at the tumor microenvironment. We propose to use this platform to determine the impact of normal and cancer associated fibroblasts and macrophages in the efficacy of MFH. These studies will provide insight to MNP specificity and MFH efficacy in multi-cellular environments. The tubeless design is suitable for both for 2D and 3D studies and is compatible with existing equipment providing a new tumor-mesenchymal model for the scientific community studying and developing therapies targeted to the tumor microenvironment.

The proposed open-well based design provides direct access for pipetting, reducing liquid shear forces commonly generated due to laminar flows within closed-well microdevices. This platform's arrangements have the potential to be easily adapted by

modifying various aspects, such as device dimensions (increasing separation between cells and/or cell seeding surface area), number of microwells, different manufacturing materials, surface treatments, and broad capabilities for cell treatment options. This study shows basic advantages of this open device model, different characterizations, and a simple design that enables cell-cell signaling and supports multi-endpoint analysis within multi-cellular *in vitro* models[9,45,46] under MFH treatment.

2.5 Cell Sub-Type Selection for Tri-culture Model of TNBC

Our previous studies have shown that MNPs targeted to the EGFR have a dramatic increase in the apoptotic levels of the TNBC cell line, MDA-MB-231 during MFH.[47] EGF-conjugated MNPs exposed to alternating magnetic fields dissipate heat locally promoting lysosome membrane permeabilization, generation of reactive oxygen species and protein precipitation. While these *in vitro* studies are highly encouraging, observations in animal studies indicate that tumor uptake of MNPs can be negatively impacted by inflammatory cells such as macrophages.[7] It has previously been shown that macrophages are capable of internalizing MNPs *in vivo* and could potentially negatively affect treatment efficacy by reducing concentrations of MNPs in localized regions.[9] However, studies in ovarian cancer using negatively-charged carboxymethyl dextran MNPs indicate that macrophages can also deliver MNPs to the tumor.[43] This contradiction is related to two main macrophage subtypes identified as M1 and M2 subtypes. Tumor-associated subtype (M2) correlates with poor prognosis and influences drug efficacy in tumor tissues. This macrophage phenotype upregulates anti-inflammatory cytokines, inhibits production of proinflammatory cytokines, participates in tissue remodeling,

regulates immune system response, and promotes survival and growth factors,[40] hence its association with tumors. Additionally, drugs have the capability of modulating the macrophage phenotype in order to influence the tumor's conduct and response to treatments.[48] For example, ferumoxytol has been shown to induce pro-inflammatory (M1 subtype) responses, inhibiting growth of adenocarcinomas, and preventing liver metastasis in mice,[25] further exhibiting macrophages' influence within a tumor microenvironment. Thus, understanding the interactions between MNPs and the tumor microenvironment *in vitro* is crucial for the optimization of the uptake of MNPs at the tumor tissue and subsequent treatment with MFH.

We proposed to develop a tri-culture model composed by breast cancer cells, fibroblasts, and macrophages. MDA-MB-231 cancer cell line has shown clinical relevance for triple negative breast tumors. NIH-3T3 fibroblasts have been used as a normal fibroblast cell line in breast cancer studies. These have shown expression of CAF-like markers in response to transforming growth factor (TGF-β) stimulus. Macrophages have been shown to carry MNPs *in vivo* thereby impacting overall distribution of MNPs among tissues and MNP uptake at tumor tissue can be affected by stromal and immune cells.[49] Our work will push clinical MNP hyperthermia treatments closer to clinical use by ascertaining the cellular response to exposure to MNPs, heat treatments, and MFH.

3 CHAPTER – OBJECTIVES

3.1 General Objective

Develop a multicellular *in vitro* model to evaluate the efficacy of MFH.

3.2 Specific Objectives

- Develop and characterize a multicellular *in vitro* model (normal and cancer model) each with epithelial, fibroblast and macrophage components.
- Compare internalization rates of MNPs in fibroblasts, macrophages and tumor cells
- Determine influence of stromal cells on the efficacy of magnetic fluid hyperthermia in tumor cells models.

4 CHAPTER – METHODOLOGY

4.1 Cell Culture

MDA-MB-231, THP-1, and NIH-3T3 cell lines were purchased from American Tissue Culture Collection (ATCC). MDA-MB-231 and NIH-3T3 were sustained by DMEM high glucose media with L-Glutamine (D5796, Sigma-Aldrich) supplemented with 10% heat inactivated fetal bovine serum (F6765, Sigma-Aldrich), 1% penicillin/streptomycin (P4333, Sigma-Aldrich). THP-1 cells were kept in RPMI 1640 (SH30027.01, GE Life Sciences) supplemented with 0.05 nM 2-mercaptoethanol (M3148, Sigma-Aldrich), 10% heat inactivated fetal bovine serum and 1% penicillin/streptomycin. All cells were maintained at 37°C in a 5% CO_2 incubator. Passages were performed at 75-80% confluence using 0.5% trypsin (59418C, Sigma-Aldrich) for adherent cells. Viable cells were counted using a cellometer through Trypan Blue exclusion (T8154, Sigma-Aldrich), subsequently diluted to the desired cell densities and seeded in microwells. These supplement concentrations were the same for all the following procedures.

4.2 THP-1 Cell Polarization

50,000 THP-1 cells were seeded in 96 well plates (701002, Nest) and were differentiated into macrophages within 48 hours using RPMI 1640 containing 36 nM PMA. Next, M1 differentiation consisted in a 48-hour incubation period in the same culture medium supplemented with 20 nM IFN-γ (300-02, PeproTech) and 10 ng/mL LPS (L4391, Sigma-Aldrich). As previously mentioned, M2 differentiation consisted in incubation with 20 ng/mL IL-4 and 20 ng/mL IL-13 RPMI for 48 hours. To determine conversion

percentage, cells were washed with PBS, incubated with 200 µL Accutase (A6964, Sigma-Aldrich) for 5-10 minutes for cell lifting, deactivated (twice) with 300 µL of RPMI 1640 supplemented with 0.05 mM 2-mercaptoethanol, 10% heat inactivated fetal bovine serum and 1% penicillin/streptomycin. Cells were transferred to sterile microtubes, centrifuged at 250g, 8°C for 5 minutes, and resuspended in 200 µL 1% bovine serum albumin (A7906, Sigma-Aldrich). Cells were then incubated with 10 µL PE Mouse Anti-Human CD206 (555954, BD Biosciences) at 4°C for 30 minutes. Lastly, cells were centrifuged again and resuspended in 50 µL PBS. Converted cells were counted through fluorescent cellometry (Vision-312-0311, Nexcelom, Lawrence, MA, USA). Negative controls included untreated THP-1 monocytes.

4.3 Polystyrene Microwell Platform Fabrication

Razor-printed culture platform components were made from polystyrene sheets and biomedical-grade adhesive tape. Briefly, microwell device preparation consists in cutting 125 µM (300711566, GoodFellow) and 190 µM (300711235, GoodFellow) polystyrene films to a desired size. The 150µm double-sided medical-grade polyester tape (90106, Adhesives Research Inc., Glen Rock, PA, USA) is then cut an additional 2 cm from the edges of the cut polystyrene sheet. Each film was joined to their own tape and, using the protruding tape, attached to a thicker sheet used as a scaffold. The scaffold was then placed in the razor printer (CE6000 Series Professional Class Cutter Plotter, Graphtec America Inc. Irvine, CA, USA) and the designs cut into the PS film and tape. The 125 µm sheet was used for to the culture regions while the 190 µm sheet for the parent well designs. Once cut, the parent wells were manually aligned and bound over

the sheet of culture regions, then placed in sterile tissue culture treated omnitrays and petri dishes. Trays were placed under ultraviolet light for 20 min in a laminar flow hood for sterilization. Figure 1 and Figure 2 show the final design for the platform and the layering involved in its manufacturing.

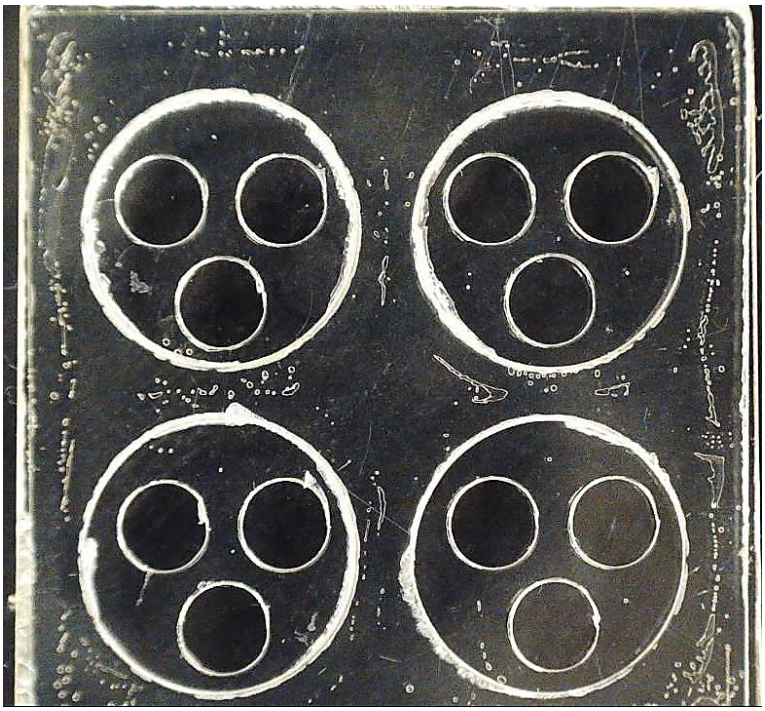

Figure 1. Polystyrene-based microwells.. This array contains four independent devices for ease of manual placement on a layer-by-layer basis.

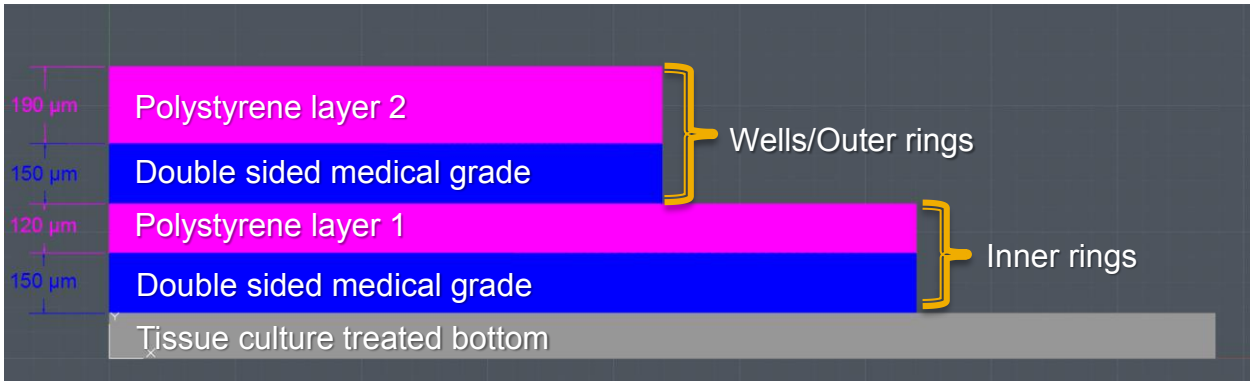

Figure 2. Transversal view of PS-based microwell device. Cells are placed directly on tissue culture treated bottom, be it glass or plastic.

4.4 Iron Oxide MNP

Carboxymethyl Dextran-coated Iron Oxide Magnetic Nanoparticles (MNPs) were prepared, characterized, and provided by Dr. Carlos Rinaldi's Lab at the Chemical Engineering Department, University of Florida-Gainesville and Dr. Madeline Torres' Lab at the Chemical Engineering Department, University of Puerto Rico-Mayagüez. DLS measurements show a MNP diameter of 63.06 nm and Magnetic Core Quantification indicates an iron core concentration of 2.97 of g/L.

4.5 Magnetic Core Quantification of Iron Oxide MNPs in Cells

Three solutions were prepared and left under agitation overnight. Hydroxylamine in DI water to 8.06 M, sodium acetate in DI water to 1.22 M and 1,10-phenathroline in DI water at 13 mM. Standards for a calibration curve were prepared at concentrations of 5.0, 4.5, 3.0, 1.5, 0.5, 0.25 µg/mL. DI water was used for no iron. MNP digestion consisted in sonication of the samples for 20 minutes, and dispensing 10µL of these in glass test tubes, adding 1 mL of nitric acid 70% to each. These were then placed in a heating block for 12 hours at 101°C. 10µL of each were then placed in a glass vial, heated to 115°C for 30 minutes, 30µL of hydroxylamine solution, 49µL of sodium acetate and 75µL of phenanthroline was added to each sample. Absorbance was measured at 508 nm in a UV-Vis Spectrophotometer (Infinite 200 Pro, Tecan Austria GmbH, Grödig, Austria).

4.6 Experimental Tri-Culture Conditions

4.6.1 Triculture Models

To compare among non-tumorigenic and tumorigenic stroma, a cancer and normal tumor cell -stromal clusters were developed. The cancer cluster consisted for M2

polarized THP-1 and TGF-β-treated NIH-3T3. The NIH-3T3 mouse fibroblast cell line was chosen as a well-established cell line model that displays a cancer-associated fibroblast phenotype in response to TGF-β[33]. THP-1 cell line was chosen due to its capability of producing large amounts of human monocytes, capable of conversion to macrophages, and subsequent polarization to varying phenotypes, including tumor-associated phenotypes[9,46,50]. The normal stroma group consists of adherent THP-1 cells (mixed M1/M2 immature phenotype) and NIH-3T3 as representative of tissue resident macrophages and fibroblasts in normal tissues. Figure 3 and Figure 4 represent the layout for the experimental setup for the devices.

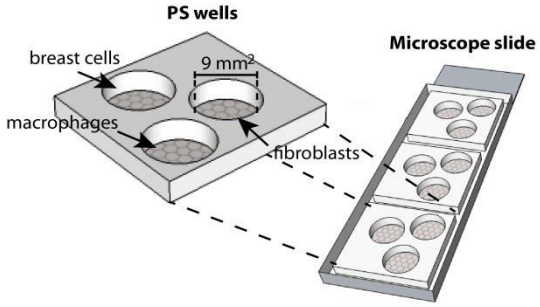

Figure 3. Schematic representation of PS platform and location of various cell types during experimentation.

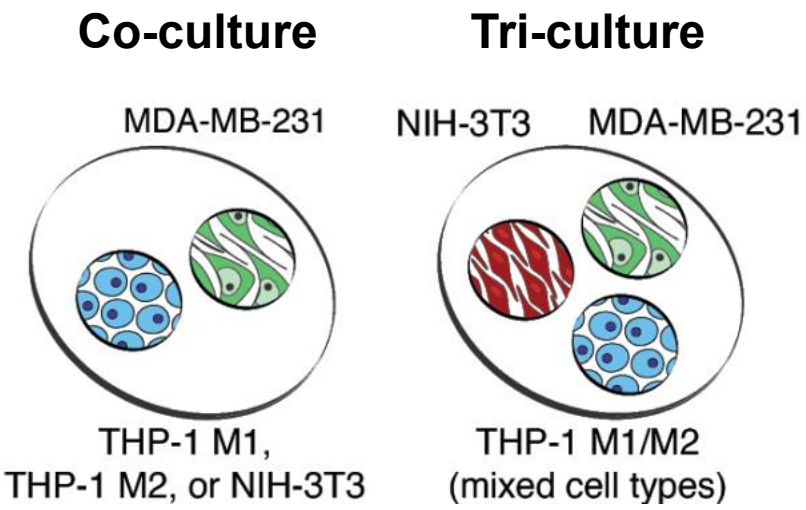

Figure 4. Co-culture and tri-culture schematic layout for varying experimental conditions. MDA-MB-231 cells were cultured in monoculture and with NIH-3T3, THP-1 or both. Layouts were used for hyperthermia and MFH.[51] *Reproduced from reference 51 with permission from Lab on a Chip and the Royal Society of Chemistry*

4.6.2 Cell Seeding in Microwells and MNP Incubation

PS micro-well geometry allows for cell seeding in adjacent yet independent compartments. A small volume of cell suspension will be enough to cover the bottom of micro-wells with cells without overfilling. As soon as cells are attached to the bottom of the culture regions, MNPs diluted in cell culture media to a concentration of 0.6 mg/mL core are added and incubated at 37°C in a 5% CO_2 incubator for two hours. MFH is then applied for 30 minutes and MNP solution is replaced with media for simultaneous interaction with all cells. After 48 hrs, cells are counted, and proliferation is assessed, both through fluorescent staining methods.

4.6.3 Hyperthermia

Cancer stroma group consisted of three cell types seeded in adjacent culture regions of an open microculture platform. Approximately 10,000 THP-1 monocytes were added in a volume of 5 µL to one microwell suspended in a mixture of cell culture medium

RPMI 1640 containing 36 ng/mL phorbol 12-myristate 13-acetate (PMA) (594400, Millipore) for differentiation to macrophages. After overnight incubation, media was replaced with RPMI 1640 media supplemented with 20 nM IL-4 (200-04, PeproTech) & IL-13 (200-13, PeproTech) for M2 phenotype polarization. Along with media replacement, approximately 4,000 NIH-3T3 cells were seeded in an adjacent microwell with 20 nM TGF-β (100-21, PeproTech) in DMEM HG (D5796, Sigma-Aldrich) medium for tumor association. In the third adjacent microwell, 4,000 MDA-MB-231 cells were seeded. For the normal stromal cluster, all cell types were seeded at the same time in each compartment. After cells have adhered to the bottom of their plates (overnight incubation), 50µL of RPMI media were overlaid on each device for effectively joining all three microwells for communication via secreted soluble factors. As a control for increase in temperature in the absence of MNPs, cells were then exposed to a fever-like temperature of 41°C in a water bath (66566, Precision Scientific, Chicago, IL, USA) for 30 minutes. Media was immediately replaced for fever and non-fever groups as the temperature upsurge may have negatively affected media components. These were then placed in the incubator for 48 hours.

4.6.4 Magnetic Fluid Hyperthermia

AMF application consists in a hollow, coiled copper tubing designed to fit a petri dish within for exposure. Chilled water flows through this tubing in order to avoid heating the copper coil and, consequently, increasing temperature through convection and affecting experimental runs. Cell setup and treatments were duplicated from the Hyperthermia Treatment section. MFH experiments were performed in Dr. Carlos

Rinaldi's laboratory at the Department of Biomedical Engineering, University of Florida-Gainesville. Experimental setup can be seen in Figure 5 and Figure 6. Addition of iron oxide MNP consisted in removal of cell culture media and addition of 750 mL DMEM at 0.6 mg/mL iron oxide core to the petri dish. Incubation with MNP lasted 2 hours for non-specific internalization. The Petri dish (Figure 7) with a four-device sticker with cells was then placed between 3rd and 4th ring in a six-turn copper coil ("Pontine", 321.3 A, 279 kHz) connected to an induction heater (Ambrell, EasyHeat, 0224). The coil and dish were inside a temperature-controlled chamber at 37°C. Temperature probes were placed on inner side of the coil and in a droplet on top of the petri dish's lid to monitor convective heating. This location was chosen to reduce the risk of contamination. Hyperthermia treatment time lasted 30 minutes for all conditions. MNP solution was removed, devices were washed with 2 mL PBS, and 2 mL DMEM were added to the dish. Proliferation was measured 48 hours after treatment.

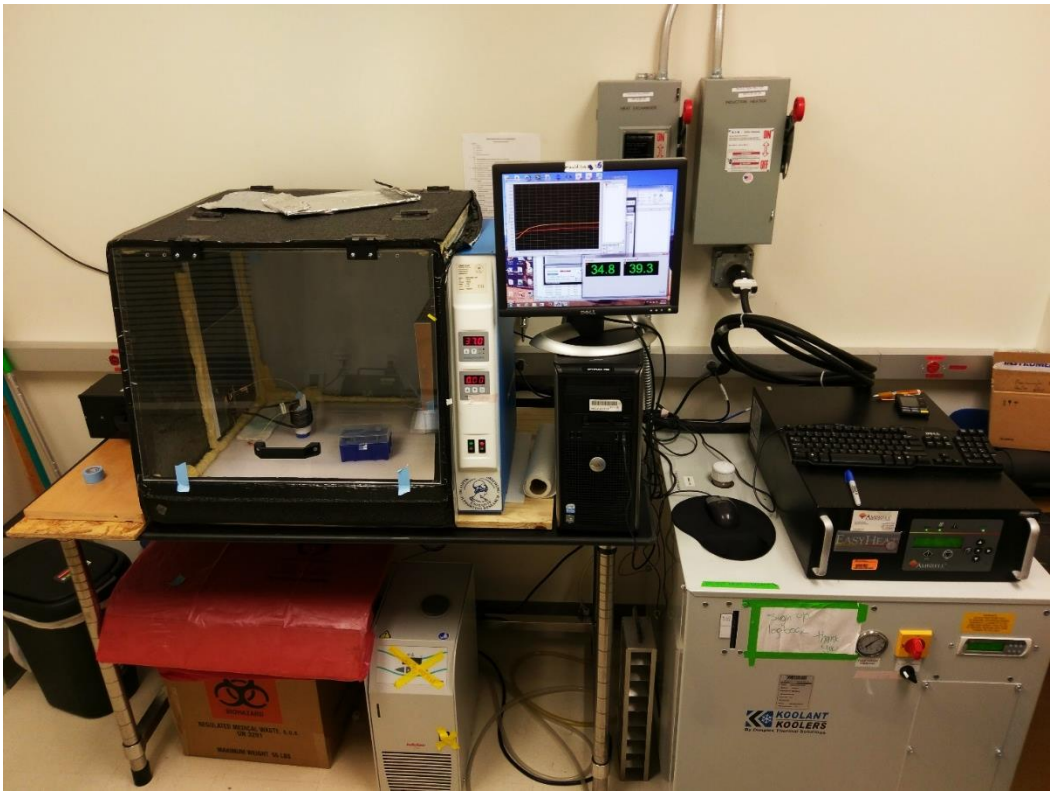

Figure 5. Experimental setup for application of MFH. Water-cooled copper "Pontine" coil sits within a temperature-controlled chamber maintained at 37°C. Recording hardware, induction heater, and water chiller sit to the right.

Figure 6. "Pontine" coil close-up. Temperature probes lie within a 35 mm^2 tissue culture treated petri dish, held by a 3D-printed plastic petri dish holder standing in the middle of the six-turn copper coil. Copper coil is cooled by recirculating water at 22°C-24°C.

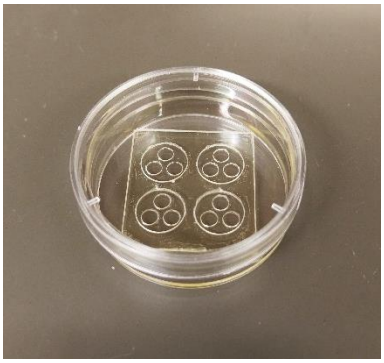

Figure 7. 35 mm^2 Petri dish used for MFH experiments. A single sticker fits in order to maximize MNP exposure to AMF, as magnetic field uniformity is reduced as coil design becomes larger.[52]

4.6.5 Cell Growth Assay

Tumor proliferation was assessed using Click-IT 594 Imaging Kit (C10639, Invitrogen) according to the manufacturer's recommendations. Hoechst 33342 (56198, BD Biosciences) nuclear staining (1:1000 dilution in PBS) was performed to obtain total cell counts. Images at 20x wide-field magnification were taken using the ZOE Fluorescent Cell Imager (Bio-Rad, Hercules, CA, USA) and cell counts were processed with ImageJ Processing and Analysis Software.[35] Proliferation fraction was determined by dividing EDU positive cell counts by the total cell counts in the tumor microwell compartment. 1-2 images were taken per microwell (30-60% of the total surface culture area) to determine fraction of proliferating cells in one 3-microwell-array. Data represents mean data average +/- 1 SE. Wilcoxon rank-sum test was performed on cell proliferation counts to report significance ($P<0.05$).

5 CHAPTER – RESULTS

5.1 Characterization of MNP

Average volumetric diameter measurements for MNP was 61nm as shown in Figure 8, A. These results were for recently manufactured MNP, other results for MNP held in storage for longer than six months indicate average volumetric diameters of 63.06nm. Proliferation assays were focused only on MDA-MB-231 triple negative breast cancer cells, since the emphasis of these experiments were on the proliferative tendencies of the tumor cells after heat and MFH treatments under varying stromal conditions.

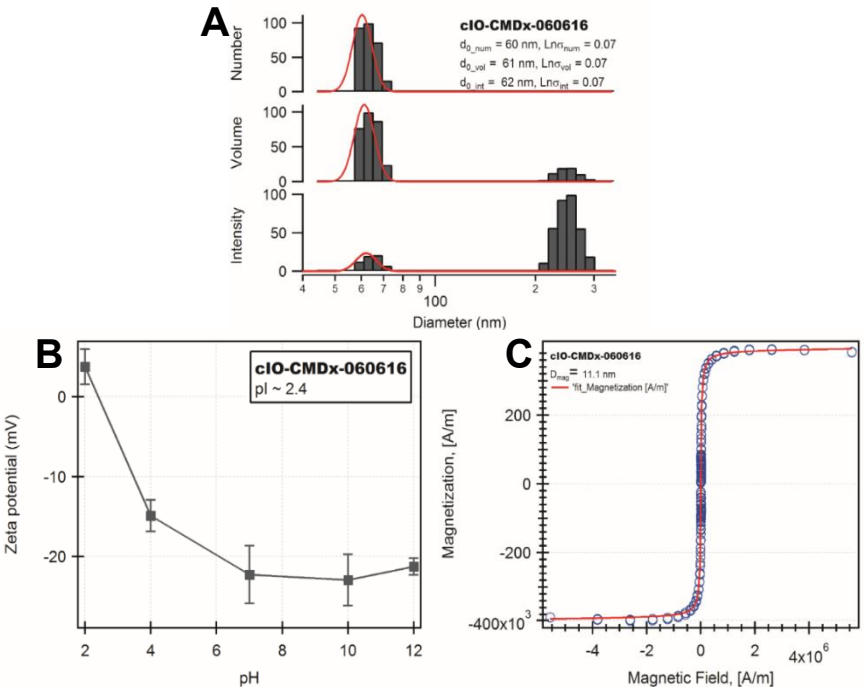

Figure 8. MNP characterization graphs. (A) Dynamic Light Scattering distribution profile indicate an average MNP diameter of 61 nm. (B) Zeta potential results confirming the net negative charge obtained through the attachment of carboxymethyl dextran. Net negative charge contributes to stability within media, allows for non-specific binding to cells, and has shown prolonged blood residence time[53]. (C) Superconducting Quantum Interference Device (SQUID) results indicate low magnetization profiles for iron oxide MNPs. This indicates superparamagnetic properties, as MNPs are magnetized only in the presence of an external magnetic field.

5.2 Cell Growth in Response to Thermal Damage

Cell proliferation results were obtained through individual cell count aided by ImageJ software. Total cell counts were obtained through the use of Hoechst staining protocol seen as blue dots noticeable in Figure 9A. On the other hand, proliferation cell counts were obtained through the use of EdU Alexa 594 staining as seen in Figure 9B. EdU binds unto newly synthesized DNA as a thymidine analogue as they proliferate. Cells are then fixed using 4% paraformaldehyde, permeabilized with 0.5% Triton X-100, followed by Alexa Fluor dye to stain proliferative cells, and finally stained with Hoechst for total cell staining and count.

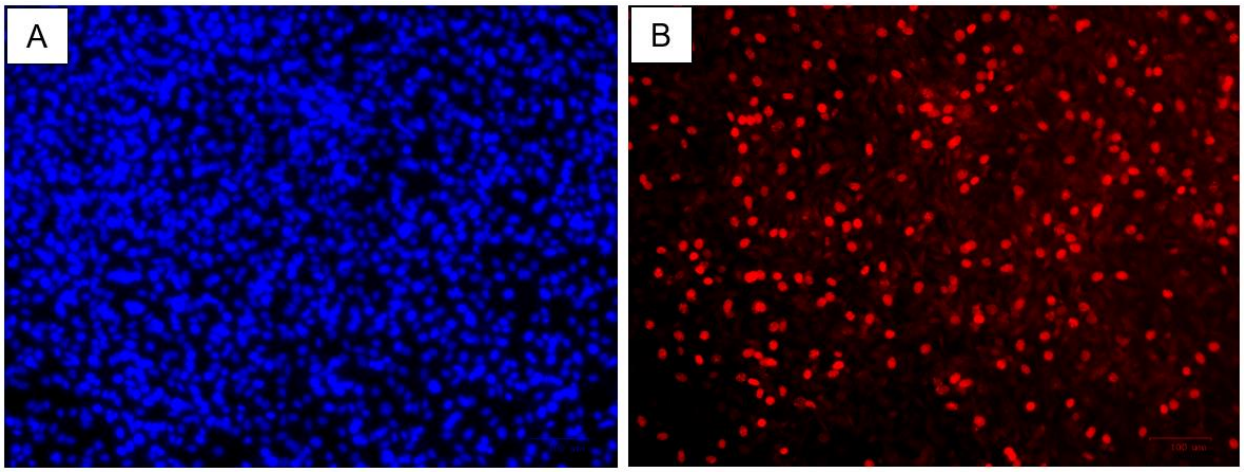

Figure 9. Click-IT EdU Proliferation Assay sample images. (A) Hoechst staining used to obtain total cell counts. (B) Alexa Fluor 594 staining used to obtain proliferative cell counts. 100 µm scale was used for both images. All images were taken using the ZOE Fluorescent Cell Imager with a wide-angle view at a 4x zoom.

Since a known concern of existing *in vitro* research is constraints towards monoculture and co-culture studies and analysis, the design used for this platform allows improvement studies involving multiple cell types within discrete cellular microenvironments. The platform opens the door for *in vitro* studies on the influence of

the stroma and matrix composition on modulating tumor cell behavior. This study in heat-induced cell death emphasizes the impact of normal and cancer stromal cell clusters in regulating cell growth and recovery rates after heat damage. Cell growth in MDA-MB-231 monocultures have been shown to be negatively affected by heat damage,[22] nevertheless, we've shown that fibroblasts and macrophages influence basal growth rates and can speed up recovery post-heat damage. This multi-cellular design allows customizable models where cancer clusters, its stroma, and the signaling between them can be assessed. Aside from evaluating tumor behavior, the host stroma and its changes can also be measured to better understand cellular crosstalk and signaling pathways in order to employ strategies to intervene within the tumor or its microenvironment. Moreover, multi-cellular models like this one are becoming more relevant in the prediction of drug efficacy.[54] The use of multi-cellular culture approaches will be of significant value to personalize medicine by providing a model to determine tumor cell response and effectiveness based on the stromal composition in the tissue.

In this application, we are modeling the use of heat which is studied as a potential adjuvant to drug therapy. Our study quantifies the sensitivity of tumor cells to heat damage in terms of cell growth and recovery rates in the presence of normal and cancer-associated stromal cell neighbors. Three different types of neighbors and their combination were studied. In agreement with previously reported observations [49], MDA-MB-231 monoculture cell growth is negatively affected by heat damage (Figure 10 A, B, C). Fibroblasts and macrophages can individually influence tumor cell growth rates and speed up recovery post-heat damage. Interestingly though, inclusion of all the cell-types

together in tri-culture had a phenotype not observed in co-culture. Instead of maintaining or promoting growth at 37°C, growth at 37°C was suppressed, yet there was a strong protective effect against heat-stress, mitigating the effect of therapy. Results such as these have significant implications for how the tumor microenvironment may perturb progression and therapeutic effects in vivo and underscore the need for engineered multicellular models to unravel the complexity of these interactions and potentially offer new approaches to increasing therapeutic efficacy. This study also illustrates the value of an open and compartmentalized culture device, providing flexible configuration, a simple user interface, and individual endpoints for each culture region.

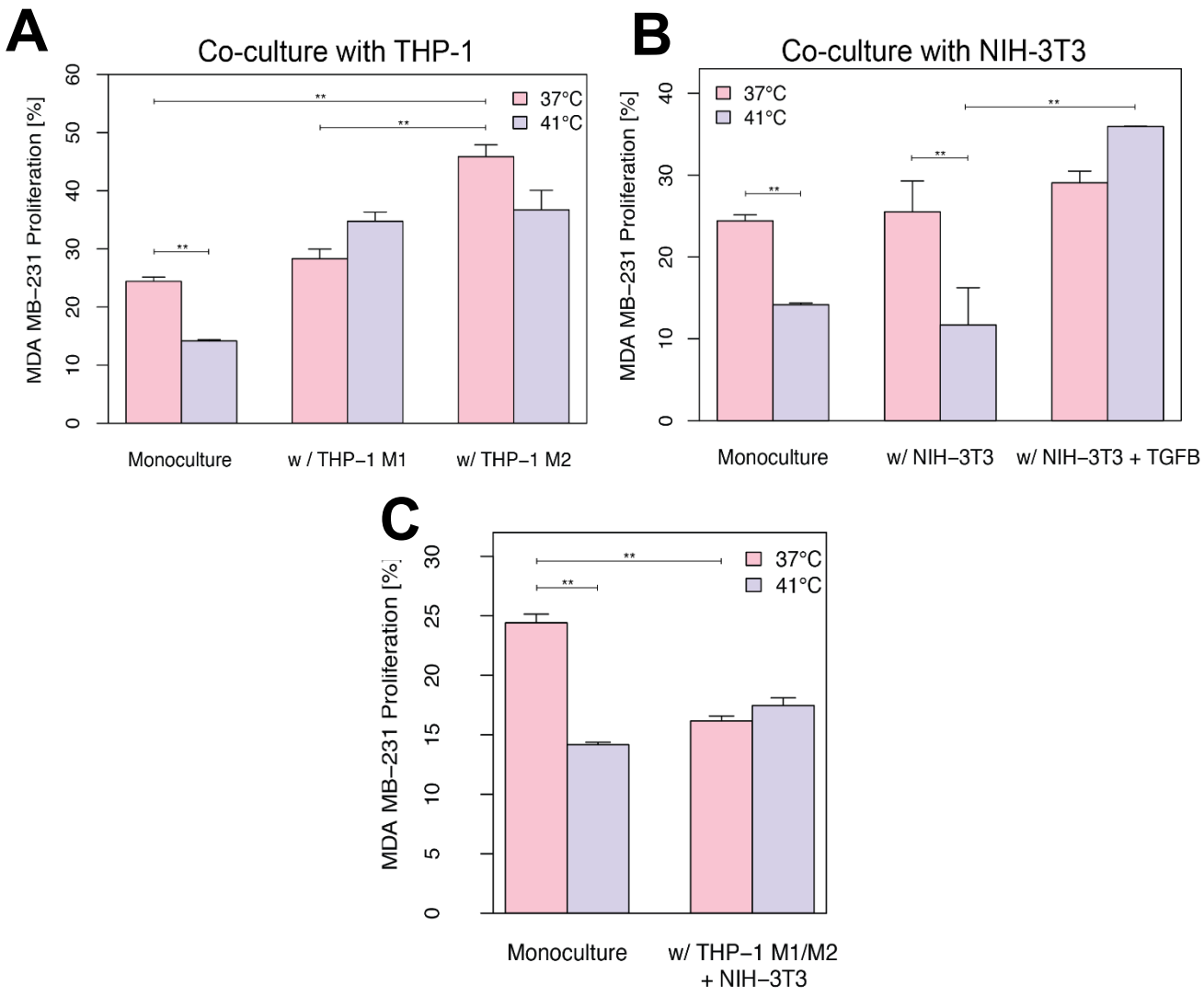

*Figure 10. Proliferation percentage for hyperthermia and MFH treatments. (A) Average MDA-MB-231 and NIH-3T3 co-culture proliferation levels after exposure to hyperthermia. Co-culture data represents average of two independent experiments with n=8 microwells. Monoculture data represents average of three independent experiments with n=4. (B) Average MDA-MB-231 and NIH-3T3 co-culture proliferation levels incubated at 37°C. Co-culture data represents average of two independent experiments with n=8 microwells. Tri-culture and monoculture data represents average of three independent experiments with n=8 and n=4 microwells, respectively. (C) Average MDA-MB-231 tri-culture proliferation levels after exposure to hyperthermia. Tri-culture and monoculture data represents average of three independent experiments with n=8 and n=4 microwells, respectively. Data from all groups represent mean data average +/- 1 SE. Wilcoxon rank-sum test, *P<0.05, **P<0.005, ***P<0.001 and **** P<0.0001.*[51]*Reproduced from reference 51 with permission from Lab on a Chip and the Royal Society of Chemistry.*

Monocultured MDA-MB-231 cancer cells suffered a significant decrease in cell proliferation when exposed to temperatures of 41°C for 30 min (Figure 10, A), as was expected. A similar, significant effect was noticeable when co-cultured with NIH-3T3 cells. A minor increase in average proliferation is observable for TGF-β+NIH-3T3, but it is not statistically significant compared with monoculture and NIH-3T3 co-culture at 37°C. A significant increase in proliferation is perceptible in MDA-MB-231 when co-cultured adjacent to TGF-β+NIH-3T3 post-heat damage. This result suggests that cancer-associated fibroblast supports MDA-MB-231 recovery after heat-stress culture conditions. When observing and comparing cancer cells' proliferation when in monoculture, co-culture, and tri-culture at 37°C (Figure 10, C), cancer-associated THP-1 M2 macrophages display increased proliferation when compared to monoculture and its M1 phenotype counterpart. MDA-MB-231 co-cultures with M2 and M1 macrophages show resistance to heat related stress, suggesting that inflammatory cells can modulate susceptibility to thermal damage in tumor cells. Results indicate that soluble factors such as paracrine and autocrine signaling have a significant influence over cell proliferation. M2 phenotype macrophages promote the recovery of tumor cells due to their promotion of anti-inflammatory (immunoregulatory capabilities) responses and pro-tumorigenic functions.[13]

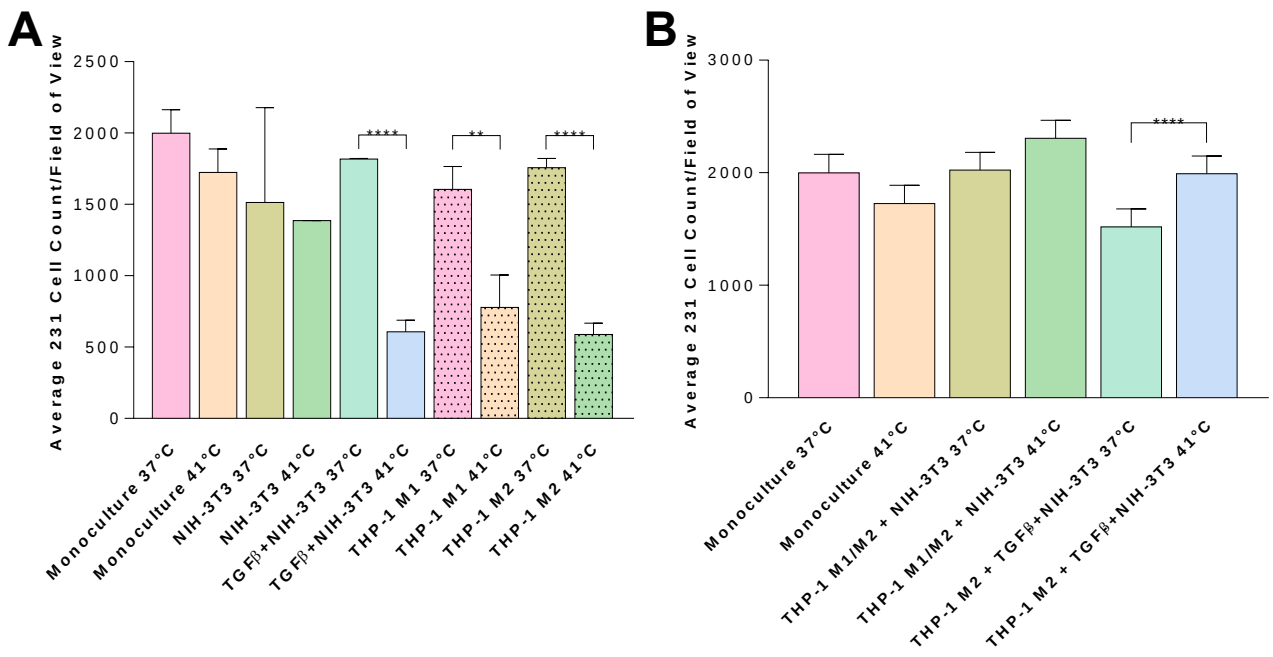

*Figure 12. Average MDA-MB-231 cell counts per field of view in co-culture and tri-culture after exposure to water bath hyperthermia. (A) Co-culture data represents average of two independent experiments with n=8 microwells. Monoculture data represents average of three independent experiments with n=4 microwells. (B) Co-culture data represents average of two independent experiments with n=8 microwells. Monoculture data represents average of three independent experiments with n=4 microwells. Data represents mean data average +/- 1 SE. Wilcoxon rank-sum test, *P<0.05, **P<0.005, ***P<0.001 and **** P<0.0001.*[51]

Cell counts for cancer-associated tri-cultures exposed to 41°C were significantly greater than when cultured at 37°C. No other significant differences were found. Figure 12, A & B present co-culture and tri-culture average cell counts, respectively. Interestingly, groups with THP-1 M2 macrophages show significantly decreased total cell counts when exposed to hyperthermia, nevertheless cancer tri-culture showed increased cell counts for the group exposed to increased temperatures.

5.3 MNP Internalization within Varying Cell Types

Linear calibration curve generated (Figure 13) was determined to be ideal for iron quantification, seeing as R-squared resulted in a value of 0.996 to R-squared. Iron

quantification results (Figure 14) showed no significant difference between M2 polarized and non-polarized macrophages. Considering that M2 polarized macrophages are not related to a pro-inflammatory response, and rather to upregulation of survival and growth factors, this would seem like the expected response.

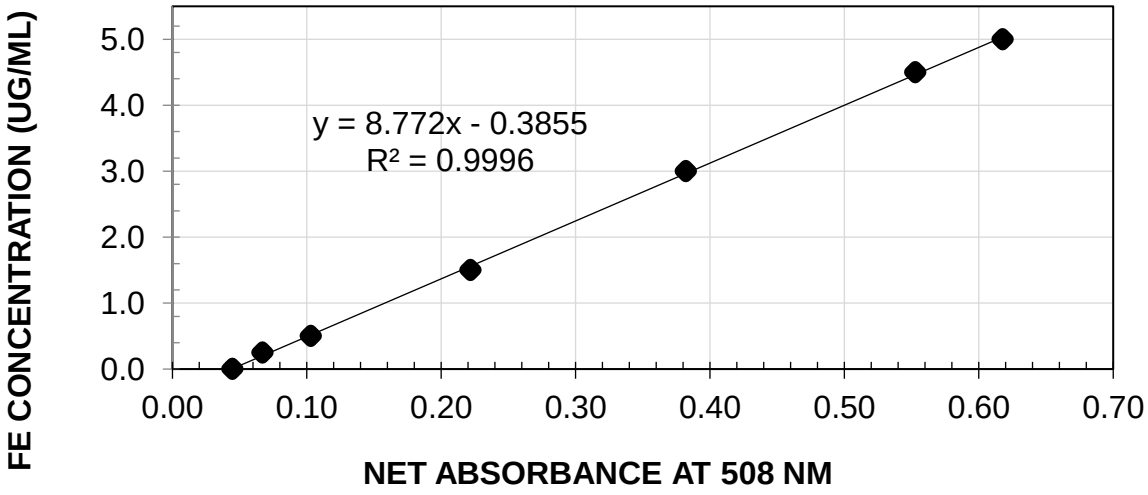

Figure 13. Calibration curve for iron quantification of internalized iron oxide nanoparticles in THP-1 macrophages.

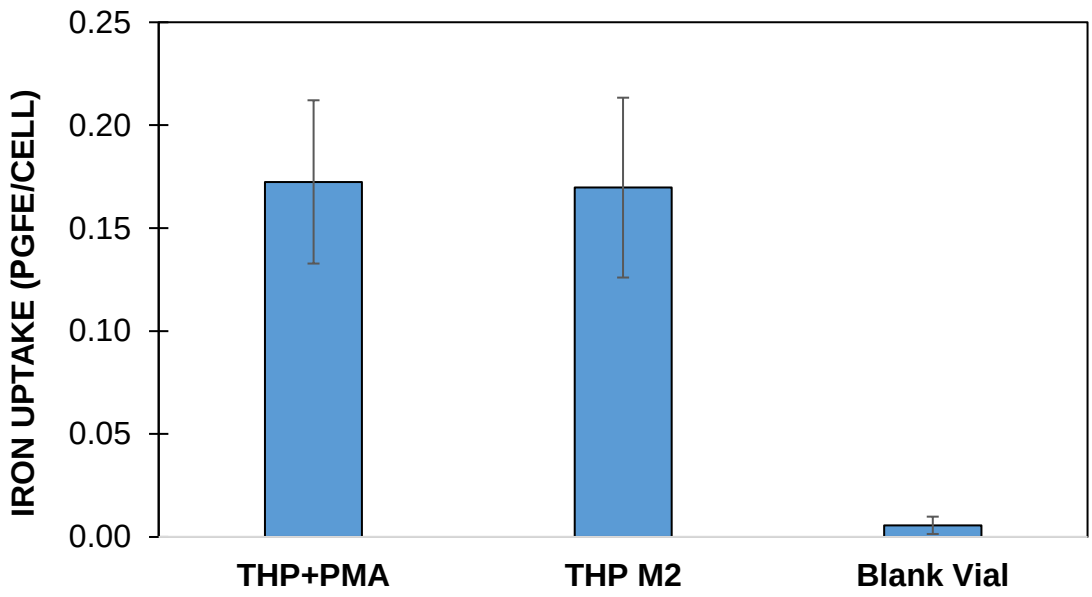

Figure 14. Iron uptake measurements for iron oxide nanoparticles within M2 polarized and non-polarized macrophages. Cells were exposed to 0.6 mg/mL core for two hours for non-specific internalization. Bars represent -/+ 1 SD.

5.4 Influence of Fibroblasts in Tumor Cell Response to MFH

The immediate objective of running a no-cell test within the induction heater was to observe the rise in temperature upon activating the alternating magnetic field and to confirm hyperthermia, observable in Figure 15. The second objective was confirming this temperature increase was mainly related to the presence of MNP within the solution and minimally related to air-liquid convection. This was achieved by avoiding the increase of water temperature over 37°C due to convective heat transfer through adjustments in the temperature of chilled water running through the copper coil. MNP solution reached a maximum of 46°C while water temperature reached a maximum of 38°C.

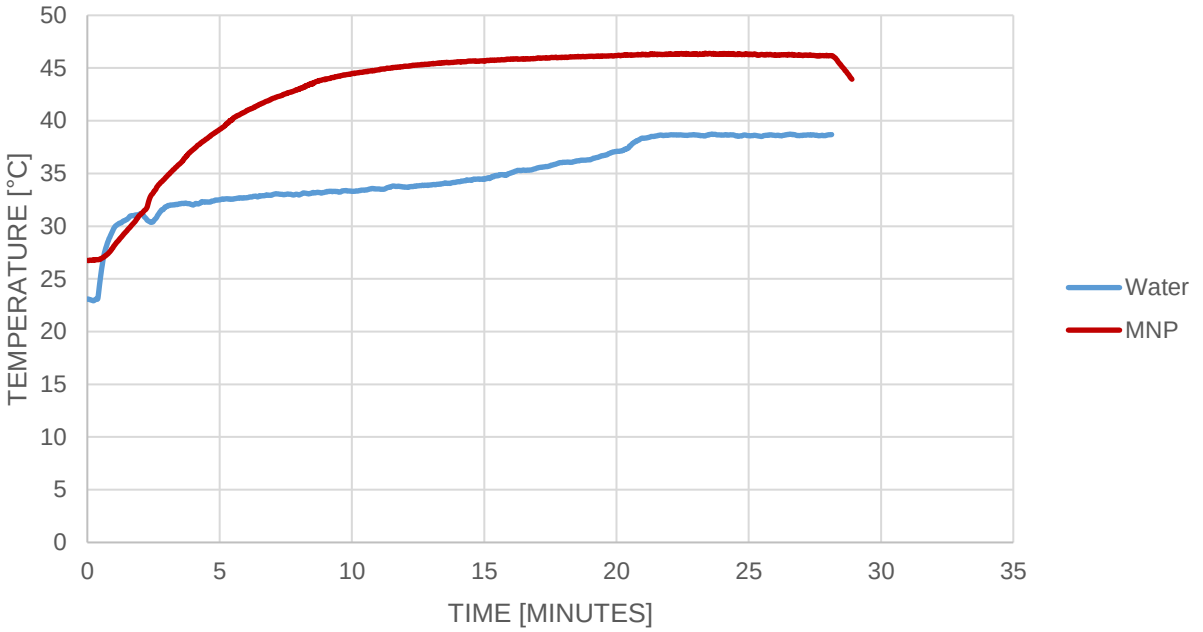

Figure 15. Temperature comparison between distilled water and 0.6 mg/mL iron oxide MNP core diluted in DMEM. MNP solution temperature reached a temperature plateau of approximately 45°C near the 12-minute mark. Maximum MNP temperature reached was 46°C, while water reached a maximum temperature of 38°C. Sudden changes in water temperature are related to adjustments in recirculating water temperatures.

Proliferation levels in MDA-MB-231 (cells labeled in S-phase) were evaluated 48 hrs post-MFH. Results (Figure 16) unexpectedly indicate proliferation levels were significantly greater ($P<0.05$) in monocultures treated with MFH as compared to non-MFH. Proliferation levels were not significantly different between Non-MFH co-culture and monoculture groups. On the other hand, when co-culture is exposed to MFH, proliferation was increased compared to non-MFH NIH-3T3 co-culture. Cancer-like fibroblasts (TGF-β+NIH-3T3) show a marginally significant increment upon exposure. Comparison of non-MFH with MFH shows no significant difference. To determine the impact of MFH in total cell number, we compared total cell counts per field of view across treatments.

MDA-MB-231 average cell count results (Figure 17) show that MFH had no effect on total cell counts except for TGF-β+NIH-3T3 co-culture group. The data suggests that cells that are resistant to heat damage have a high proliferative capacity, which is supported by the adjacent stroma phenotype. Our results support the stroma as a regulator of tumor cell recovery from heat damage and protector of tumor cell sub-types with high regenerative capacity.

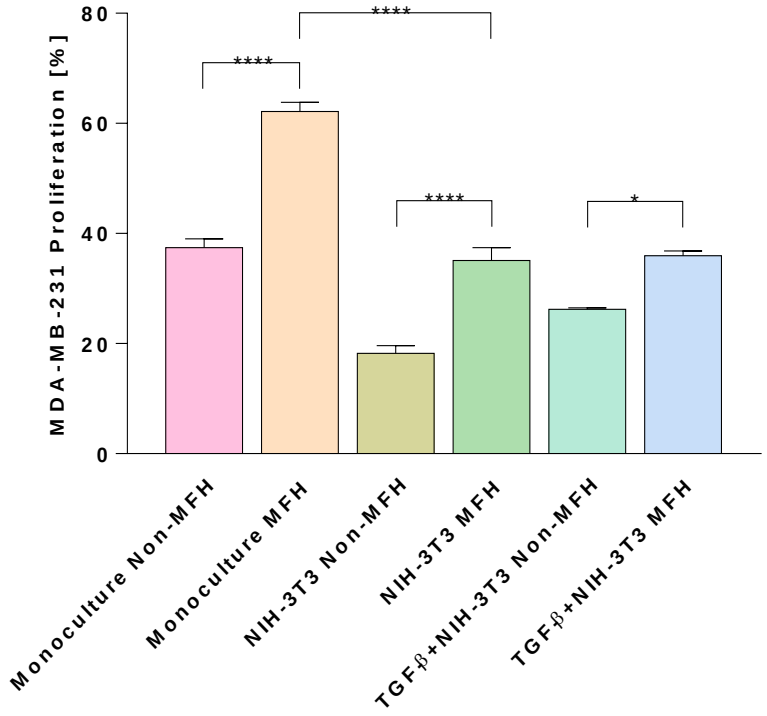

*Figure 16. Proliferation percentage for monoculture and co-culture MFH treatments. Average MDA-MB-231 proliferation after exposure to heat damage through MFH. MNP incubation lasted 2 hours, cells were cultured at 37°C or exposed to AMF for 30 min. Monoculture data represents average of 3 independent experiments with n=8. Monoculture Non-MFH and MFH represents average of two independent experiments with n=16. Co-culture data represents average of dual independent experiments with n=8. Data from all groups represent mean data average +/- 1 SE. Wilcoxon rank-sum test, *P<0.05, **P<0.005, ***P<0.001 and **** P<0.0001.*

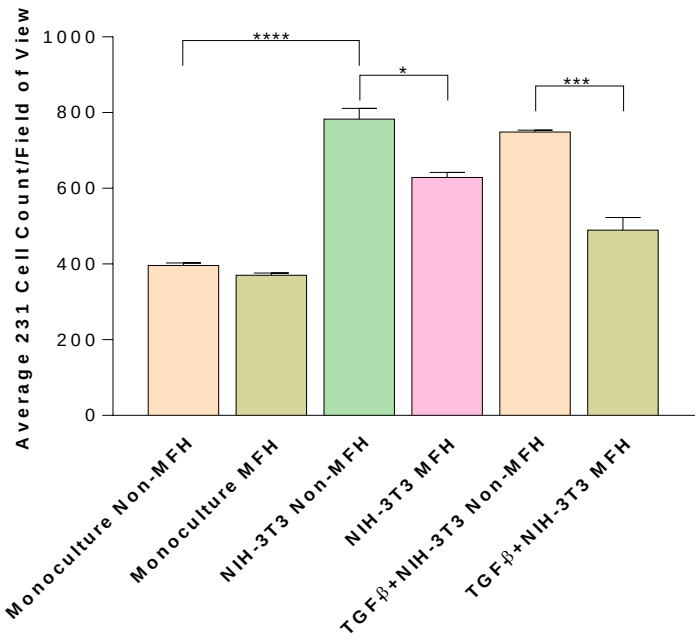

*Figure 17. Comparison of cell counts per field of view of normal and cancer-related conditions for monoculture and co-culture cell counts under MFH. Monoculture and co-culture data represent average of dual independent experiments with n=16 and n=8, respectively. Data represents mean data average +/- 1 SE. Wilcoxon rank-sum test, *P<0.05, **P<0.005, ***P<0.001 and **** P<0.0001.*

6 CHAPTER – CONCLUSION

Cell growth and recovery processes are influenced by the presence of additional cells, those of which compose the stroma and sculpt the microenvironment. Findings clearly show that soluble signals are being transmitted through the cell media, provoking the tumor cells to have a specific response to fibroblasts and macrophages. Particularly, macrophages have already been shown to influence the performance of varying cell types and their response to external agents.

Microfluidic devices such as ours can clearly be used as a comprehensive tool to obtain a complete depiction of soluble signaling and MFH treatment influence. The techniques utilized here will be further developed in order to determine additional factors influencing TNBC. This work will push clinical MNP hyperthermia treatments closer to clinical use by ascertaining the role macrophages have amongst normal and cancerous cells under therapy. The data obtained in this study can be subsequently utilized for additional research into different types of cells to continue observations into multicellular interactions for cancer.

Future work will be needed to compare proliferation levels in cell-targeted and non-targeted MNP within normal and cancerous clusters. Additionally, uptake and internalization levels will be measured within macrophages with differing phenotypes in monoculture and multicellular environments to assess treatment resistance. Related work could be performed to determine protein expression levels of paracrine and autocrine signaling associated with tissue inflammation, heat-related trauma, and cluster recovery.

Some of these studies will be able to be supported by a next generation co-culture device, which encompasses a larger area for greater cell seeding capacity and increased capabilities for biomolecule detection.

REFERENCES

1. Quail, D. F. & Joyce, J. A. Microenvironmental regulation of tumor progression and metastasis. *Nat. Med.* **19,** 1423–37 (2013).

2. Müller, a *et al.* Involvement of chemokine receptors in breast cancer metastasis. *Nature* **410,** 50–6 (2001).

3. Metallo, C. M. *et al.* Engineering the stem cell microenvironment. *Biotechnol. Prog.* **23,** 18–23 (2007).

4. Domenech, M. *et al.* Cellular observations enabled by microculture: paracrine signaling and population demographics. *Integr. Biol.* **1,** 267 (2009).

5. Weigelt, B. & Bissell, M. J. Unraveling the microenvironmental influences on the normal mammary gland and breast cancer. *Semin. Cancer Biol.* **18,** 311–321 (2008).

6. Creixell, M., Bohórquez, A. C., Torres-Lugo, M. & Rinaldi, C. EGFR-targeted magnetic nanoparticle heaters kill cancer cells without a perceptible temperature rise. *ACS Nano* **5,** 7124–7129 (2011).

7. Court, K. A. *et al.* HSP70 Inhibition Synergistically Enhances the Effects of Magnetic Fluid Hyperthermia in Ovarian Cancer. *Mol. Cancer Ther.* **16,** 966–976 (2017).

8. Regehr, K. J. *et al.* Biological implications of polydimethylsiloxane-based microfluidic cell culture. *Lab Chip* **9,** 2132–2139 (2009).

9. Genin, M., Clement, F., Fattaccioli, A., Raes, M. & Michiels, C. M1 and M2 macrophages derived from THP-1 cells differentially modulate the response of cancer cells to etoposide. *BMC Cancer* **15,** 577 (2015).

10. Aysola, K. *et al.* Triple Negative Breast Cancer – An Overview. **2013,** 1–7 (2014).

11. Liu, B. *et al.* Metformin induces unique biological and molecular responses in triple negative breast cancer cells. *Cell Cycle* **8,** 2031–2040 (2009).

12. Domenech, M. & Marrero-Berrios, I. Lysosomal membrane permeabilization by targeted magnetic nanoparticles in alternating magnetic fields. *Acs …* **7,** 5091–5101 (2013).

13. Zanganeh, S. *et al.* Iron oxide nanoparticles inhibit tumour growth by inducing pro-inflammatory macrophage polarization in tumour tissues. *Nat. Nanotechnol.* (2016). doi:10.1038/nnano.2016.168

14. Tran, N. & Webster, T. J. Magnetic nanoparticles: biomedical applications and challenges. *J. Mater. Chem.* **20,** 8760 (2010).

15. Reddy, L. H., Arias, J. L., Nicolas, J. & Couvreur, P. Magnetic nanoparticles: Design and characterization, toxicity and biocompatibility, pharmaceutical and biomedical applications. *Chem. Rev.* **112,** 5818–5878 (2012).

16. Mcnamara, K., Tofail, S. A. M., Mcnamara, K. & Tofail, S. A. M. Advances in Physics : X Nanoparticles in biomedical applications. *Adv. Phys. X* **2,** 1–35 (2017).

17. Seemann, K. M. *et al.* Magnetic heating properties and neutron activation of

tungsten-oxide coated biocompatible FePt core-shell nanoparticles. *J. Control. Release* (2014). doi:10.1016/j.jconrel.2014.11.007

18. Stocke, N. A. *et al.* Toxicity evaluation of magnetic hyperthermia induced by remote actuation of magnetic nanoparticles in 3D micrometastasic tumor tissue analogs for triple negative breast cancer. *Biomaterials* **120,** 115–125 (2017).

19. Laurent, S., Dutz, S., Häfeli, U. O. & Mahmoudi, M. Magnetic fluid hyperthermia: Focus on superparamagnetic iron oxide nanoparticles. *Adv. Colloid Interface Sci.* **166,** 8–23 (2011).

20. Maier-Hauff, K. *et al.* Efficacy and safety of intratumoral thermotherapy using magnetic iron-oxide nanoparticles combined with external beam radiotherapy on patients with recurrent glioblastoma multiforme. *J. Neurooncol.* **103,** 317–324 (2011).

21. Tartaj, P. The preparation of magnetic nanoparticles for applications in biomedicine. *J. Phys. D …* **182,** (2003).

22. Obaidat, I., Issa, B. & Haik, Y. Magnetic Properties of Magnetic Nanoparticles for Efficient Hyperthermia. *Nanomaterials* **5,** 63–89 (2015).

23. Li, J. *et al.* Carboxymethylated Dextran-Coated Magnetic Iron Oxide Nanoparticles for Regenerable Bioseparation. *J. Nanosci. Nanotechnol.* **11,** 10187–10192 (2011).

24. Rovers, S. A., Hoogenboom, R., Kemmere, M. F. & Keurentjes, J. T. F. Relaxation processes of superparamagnetic iron oxide nanoparticles in liquid and incorporated in poly(methyl methacrylate). *J. Phys. Chem. C* **112,** 15643–15646 (2008).

25. Schneider, C. A., Rasband, W. S. & Eliceiri, K. W. NIH Image to ImageJ : 25 years of image analysis HISTORICAL commentary NIH Image to ImageJ : 25 years of image analysis. *Nat. Methods* **9,** 671–675 (2012).

26. Crown, J., O'Shaughnessy, J. & Gullo, G. Emerging targeted therapies in triple-negative breast cancer. *Ann. Oncol.* **23,** (2012).

27. Kathryn, J. C., Sireesha V, G. & Stanley, L. Triple Negative Breast Cancer Cell Lines: One Tool in the Search for Better Treatment of Triple Negative Breast Cancer. *Breast Dis* **32,** 35–48 (2012).

28. Quinto, C. A., Mohindra, P., Tong, S. & Bao, G. Multifunctional superparamagnetic iron oxide nanoparticles for combined chemotherapy and hyperthermia cancer treatment. *Nanoscale* **7,** 12728–12736 (2015).

29. Kozissnik, B., Bohorquez, A. C., Dobson, J. & Rinaldi, C. Magnetic fluid hyperthermia: Advances, challenges, and opportunity. *Int. J. Hyperth.* **29,** 706–714 (2013).

30. Lacava, L. M. *et al.* Use of magnetic resonance to study biodistribution of dextran-coated magnetic fluid intravenously administered in mice. *J. Magn. Magn. Mater.* **252,** 367–369 (2002).

31. Gustafson, H. H., Holt-Casper, D., Grainger, D. W., Ghandehari, H. & Grainger, D. Nanoparticle Uptake: The Phagocyte Problem HHS Public Access. *Nano Today* **10,** 487–510 (2015).

32. Wilhelm, S. *et al.* Analysis of Nanoparticle Delivery to Tumours. *Nat. Rev. Mater.* **1,**

1–138 (2016).

33. Bhowmick, N. A., Neilson, E. G. & Moses, H. L. Stromal fibroblasts in cancer initiation and progression. *Nature* **432,** 332–337 (2004).

34. Stallcop, L. *et al.* Razor-printed sticker microdevices for cell-based applications. *Lab Chip* (2018). doi:10.1039/C7LC00724H

35. Benton, G., Ph, D., George, J. & Ph, D. Extracellular Matrix Proteins for Triculture of Breast Cancer Spheroids , Endothelial Tubules and Human Mesenchymal Stem Cells. **44,** 1–6

36. Pagani, S. *et al.* An advanced tri-culture model to evaluate the dynamic interplay among osteoblasts, osteoclasts, and endothelial cells. *J. Cell. Physiol.* **233,** 291–301 (2018).

37. Bruce, A. *et al.* Three-dimensional microfluidic tri-culture model of the bone marrow microenvironment for study of acute lymphoblastic leukemia. *PLoS One* **10,** 1–16 (2015).

38. Wang, I.-N. E. *et al.* Cellular interactions regulate stem cell differentiation in tri-culture. *Connect. Tissue Res.* **57,** 476–487 (2016).

39. Barkal, L. J. *et al.* Microbial volatile communication in human organotypic lung models. *Nat. Commun.* **8,** (2017).

40. Lee, J. H. *et al.* Exchange-coupled magnetic nanoparticles for efficient heat induction. *Nat. Nanotechnol.* **6,** 418–422 (2011).

41. Fischer, H. C., Hauck, T. S., Gómez-Aristizábal, A. & Chan, W. C. W. Exploring primary liver macrophages for studying quantum dot interactions with biological systems. *Adv. Mater.* **22,** 2520–2524 (2010).

42. Regier, M. C., Alarid, E. T. & Beebe, D. J. Progress towards understanding heterotypic interactions in multi-culture models of breast cancer. *Integr. Biol.* **8,** 684–692 (2016).

43. Domenech, M., Bjerregaard, R., Bushman, W. & Beebe, D. J. Hedgehog signaling in myofibroblasts directly promotes prostate tumor cell growth. *Integr. Biol.* **4,** 142 (2012).

44. Byrne, M. B., Leslie, M. T., Patel, H. S., Gaskins, H. R. & Kenis, P. J. A. Design considerations for open-well microfluidic platforms for hypoxic cell studies. *Biomicrofluidics* **11,** (2017).

45. Través, P. G., Luque, A. & Hortelano, S. Macrophages, inflammation, and tumor suppressors: ARF, a new player in the game. *Mediators Inflamm.* **2012,** (2012).

46. Wang, X., Zhao, X., Wang, K., Wu, L. & Duan, T. Interaction of monocytes/macrophages with ovarian cancer cells promotes angiogenesis in vitro. *Cancer Sci.* **104,** 516–523 (2013).

47. Chao, Y. *et al.* Recognition of dextran-superparamagnetic iron oxide nanoparticle conjugates (feridex) via macrophage scavenger receptor charged domains. *Bioconjug. Chem.* **23,** 1003–1009 (2012).

48. Zanganeh, S. *et al.* Iron oxide nanoparticles inhibit tumour growth by inducing pro-

inflammatory macrophage polarization in tumour tissues. *Nat. Nanotechnol.* **11,** 986–994 (2016).

49. Thompson, E. A. *et al.* Differential response of MCF7, MDA-MB-231, and MCF 10A cells to hyperthermia, silver nanoparticles and silver nanoparticle-induced photothermal therapy. *Int. J. Hyperth.* **30,** 312–323 (2014).

50. Tjiu, J.-W. *et al.* Tumor-associated macrophage-induced invasion and angiogenesis of human basal cell carcinoma cells by cyclooxygenase-2 induction. *J. Invest. Dermatol.* **129,** 1016–1025 (2009).

51. Alvarez-Garcia, Yasmin Rosaura, Karla P. Ramos-Cruz, Reinaldo J. Agostini-Infanzón, Loren E. Stallcop, David J. Beebe, Jay W. Warrick, M. D. Open multi-culture platform for simple and flexible study of multi-cell type interactions. *Lab Chip* (2018).

52. Jeon, J. S. *et al.* Correction for Jeon et al., Human 3D vascularized organotypic microfluidic assays to study breast cancer cell extravasation. *Proc. Natl. Acad. Sci.* **112,** E818–E818 (2015).

53. Laurent, S. *et al.* Magnetic Iron Oxide Nanoparticles: Synthesis, Stabilization, Vectorization, Physicochemical Characterizations, and Biological Applications (vol 108, pg 2064, 2008). *Chem. Rev.* **108,** 2064–2110 (2008).

54. Qin, Z. The use of THP-1 cells as a model for mimicking the function and regulation of monocytes and macrophages in the vasculature. *Atherosclerosis* **221,** 2–11 (2012).